Mechanism of an Alkyl-Dependent Photochemical Homolysis of the Re–Alkyl Bond in [Re(R)(CO)$_3$(α-diimine)] Complexes via a Reactive σπ* Excited State

Brenda D. Rossenaar, Cornelis J. Kleverlaan, Maartje C. E. van de Ven, Derk J. Stufkens*, and Antonín Vlček, Jr.*

Abstract: MLCT excitation of the complexes [Re(R)(CO)$_3$(α-diimine)] (R = Me, Et, benzyl (Bz); α-diimine = *i*Pr-PyCa, R′-DAB) results in the homolysis of the Re–R bond leading to the formation of radicals R$^\bullet$ and [Re(CO)$_3$(α-diimine)]$^\bullet$ as primary photoproducts. The quantum yield of this photoprocess is dependent on the alkyl group used. For R = Me, the quantum yield is low (10^{-2}) and depends on the temperature and excitation wavelength, whereas for R = Et and Bz the quantum yield is near unity and independent of T and λ_{exc}. The reaction is shown to proceed via a σ(Re–R)π* excited state that is rapidly (< 20 ps) populated by a nonradiative transition from the optically excited MLCT state. Time-resolved IR and UV/Vis absorption spectra studied in the ns–μs and ps–μs time domains, respectively, show that the σπ* excited state is rather long-lived (τ ≈ 250 ns) in noncoordinating solvents; the dissociation of the Re–R bond from this state is strongly accelerated by polar or coordinating solvents ($\tau_{\sigma\pi^*} < 20$ ps). The σπ* excited state is spectroscopically characterized by a (presumably σπ* → MLCT) transition at approximately 500 nm and by CO stretching frequencies closely resembling their ground-state values. The relative energies of the MLCT and reactive σπ* states, controlled by the nature of the alkyl ligand, determine the photoreactivity of the complexes.

Keywords
homolytic cleavage · organometallic compounds · photochemistry · rhenium complexes · time-resolved spectroscopy

Introduction

Organometallic complexes containing an α-diimine ligand bound to a low-valent metal atom have been the subject of numerous photochemical and photophysical studies.[1–5] Most of their intriguing photoactivity, for example long-lived emission and excited-state electron transfer, originates in the $d_\pi \rightarrow$ α-diimine metal-to-ligand charge transfer (MLCT) excited states. An interesting situation arises when such an MLCT-active α-diimine complex contains another ligand that is bound covalently to the metal atom by a relatively high-energy σ orbital. Such metal–ligand bonds are often prone to homolytic splitting. Hence, optical excitation of these mixed-ligand complexes is expected to initiate a very interesting photoreactivity. Indeed, homolytic splitting occurs upon MLCT excitation of metal–metal bonded complexes [L$_n$MM′(CO)$_3$(α-diimine)] (L$_n$M = (CO)$_5$M′, Ph$_3$Sn, (CO)$_4$Co, etc.; M′ = Mn, Re)[6–17] and [L$_n$MRu(Me)(CO)$_2$(α-diimine)],[18, 19] or metal–alkyl complexes [ZnR$_2$(α-diimine)],[20] [Pt(Me)$_4$(α-diimine)],[21, 22] [Ir(R)(CO)$_2$(PAr$_3$)$_2$(mnt)],[23] [Ru(X)(R)(CO)$_2$(α-diimine)][24, 25] and [M(R)(CO)$_3$(α-diimine)] (M = Mn, Re).[26–28]

In principle, visible excitation of these complexes may lead to the occupation of either the MLCT or the σπ* excited state. However, only in the cases of [ZnR$_2$(α-diimine)][20] and [Pt(Me)$_4$(α-diimine)][21] has direct population of the σπ* excited state by optical excitation been observed. In all other cases, direct optical population of the σπ* excited state is prevented by the fact that the σ → π* spectral transition is overlap-forbidden and thus has only rather small oscillator strength. The σπ* excited state may then only be populated indirectly by a nonradiative transition from the MLCT excited state; it has been proposed that this occurs after visible excitation of several of the complexes mentioned above.[14, 19, 25, 27] The intense MLCT transition then functions as a very efficient input of optical energy in the reactive molecule. Which excited state is populated and which deactivation pathway is followed (e.g., decay to the ground state, homolysis of the σ bond, heterolytic release of a ligand) are determined among other factors by the relative energies of the σ orbital and the filled d_π orbitals of the complex, which, in turn, are strongly dependent on the nature of the ligands.

The versatile ligand-dependent excited-state behaviour of mixed-ligand α-diimine complexes has been clearly demonstrated for the [Ru(X)(R)(CO)$_2$(α-diimine)] complexes.[24, 29, 30] Changing X from Cl to I to Mn(CO)$_5$ caused the excited-state behaviour to change from typically MLCT to I → α-diimine XLCT to σπ*, respectively. Also the alkyl R had a profound

[*] Prof. Dr. D. J. Stufkens, Dr. B. D. Rossenaar, C. J. Kleverlaan, M. C. E. van de Ven
Anorganisch Chemisch Laboratorium, J. H. van 't Hoff Research Institute
Universiteit van Amsterdam, Nieuwe Achtergracht 166
1018 WV Amsterdam (The Netherlands)
Telefax: Int. code +(20) 525-6456
e-mail: inorg.chem@sara.nl
Dr. A. Vlček, Jr.
J. Heyrovský Institute of Physical Chemistry
Academy of Sciences of the Czech Republic
Dolejškova 3, 182 23 Prague (Czech Republic)

0947-6539/96/0202-0228 $ 10.00+.25/0

influence on the excited-state behaviour. For X = halide and R = Me or Et, the complexes were photostable, whereas the *i*-propyl complexes decomposed into radicals by homolysis of the Ru–*i*Pr bond.[25] Apparently, the relative energies of the MLCT and σπ* excited states depend on R, and the reactive σπ* state can only be reached for R = *i*Pr.

We have observed a similar dependence of the excited-state behaviour on R for the complexes [Mn(R)(CO)$_3$(R′-DAB)] (R = Me, Bz).[27] For R = Me, release of CO was observed upon visible excitation, whereas for R = Bz homolysis of the Mn–Bz bond resulting in the formation of radicals was observed. Also in this case, the excited-state behaviour observed could be explained with the relative energies of the MLCT and σπ* states. For R = Me, the MLCT state is the lowest-energy excited state, whereas for R = Bz the σπ* state is populated nonradiatively after excitation into the MLCT absorption band.

Recently, we have prepared and characterized[31] a series of complexes [Re(R)(CO)$_3$(α-diimine)] (R = Me, Et, Bz; α-diimine = pyridine-2-carbaldehyde-*N*-isopropylimine (*i*Pr-PyCa), *N*,*N*′-diorgano-1,4-diaza-1,3-butadiene (R′-DAB)). The structures of these complexes and of the α-diimine ligands used are depicted in Figure 1.

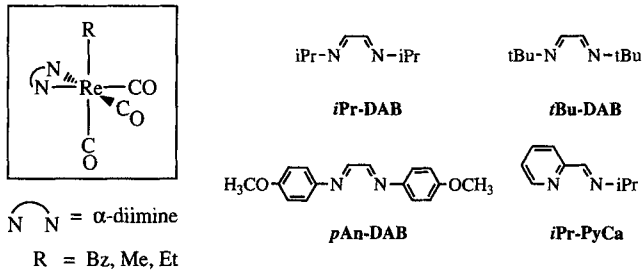

Fig. 1. Structures of the complexes [Re(R)(CO)$_3$(α-diimine)] and ligands used.

Preliminary experiments on some of these compounds have immediately pointed to their intriguing photochemical behaviour.[28, 32] Hence, in order to gain more insight into the delicate properties of the σπ* excited state, we have investigated the photochemical reactivity of these complexes as well as their excited-state dynamics in the picosecond-to-nanosecond time domain as a function of the α-diimine and R ligands in different solvents and at various temperatures. This study allows us to draw more general conclusions on the structural factors that determine the properties and reactivity of the, often elusive, σπ* state, as well as on the mechanism of its population. Hence, a better understanding of the photochemical activation of metal–carbon bonds may be achieved.

Results

Photochemistry: All [Re(R)(CO)$_3$(α-diimine)] complexes under study are more or less photoreactive upon irradiation into their MLCT absorption bands. The photochemical reactivity of the complexes was followed in situ by IR, UV/Vis and ^{1}H NMR spectroscopy in different solvents.

In neat CCl_4, all complexes underwent a thermal reaction with the solvent, resulting in the formation of [Re(Cl)(CO)$_3$(α-diimine)]. However, in $CHCl_3$ or CH_2Cl_2, most complexes were thermally stable and afforded [Re(Cl)(CO)$_3$(α-diimine)] only upon irradiation into the MLCT absorption band. When this reaction was followed for [Re(Bz)(CO)$_3$(*i*Pr-DAB)] in situ with ^{1}H NMR by means of a CIDNP probe in which the sample was irradiated through a fibre, the signals of the starting material disappeared and new signals from [Re(Cl)(CO)$_3$(*i*Pr-DAB)] grew in. In addition, signals of dibenzyl appeared at $\delta = 7.3$ (m) and 2.94 (s), as well as signals of toluene (in a ratio of 3:1). The GCMS analysis of the organic products also showed the formation of dibenzyl and toluene. All other complexes [Re(R)(CO)$_3$(α-diimine)] discussed in this paper underwent a similar reaction to yield the chloro complex, as is clear from comparison of the IR and UV/Vis spectra of the photoproduct with the data for authentic [Re(Cl)(CO)$_3$(α-diimine)] complexes.[33] The photoreactivity of the methyl complexes was always much lower than that of their ethyl and benzyl congeners.

All these results suggest that the Re–alkyl bond is split homolytically upon irradiation, resulting in alkyl radicals and [Re(CO)$_3$(α-diimine)]$^\bullet$ radicals, according to Equation (1).

$$[Re(R)(CO)_3(\alpha\text{-diimine})] \xrightarrow{h\nu} [Re(CO)_3(\alpha\text{-diimine})]^\bullet + R^\bullet$$
$$\xrightarrow{CH_2Cl_2} [Re(Cl)(CO)_3(\alpha\text{-diimine})] + R_2/RH \quad (1)$$

Irradiation in THF, 2-MeTHF, toluene etc. in the absence of a radical scavenger such as a Cl-donating solvent resulted in a more complex product formation. The spectroscopic data of the products formed upon photolysis in THF together with relevant literature data are collected in Table 1. The IR spectral changes observed during the photolysis of the complexes indicated that at room temperature two major types of products were formed in these solvents. For example, irradiation of [Re(Et)(CO)$_3$(*i*Pr-PyCa)] in THF led to a product A that has CO stretching frequencies at 2002, 1888 and 1875 cm^{-1}, and to a second product B with CO stretching frequencies at 2021, 1918 and 1891 cm^{-1}. In some cases other CO-containing by-products were formed in low concentrations. Those by-products were not further investigated. When the temperature was lowered to

Table 1. IR $\tilde{\nu}$(CO) frequencies and UV/Vis absorption maxima of the major photoproducts of [Re(R)(CO)$_3$(α-diimine)] in THF at room temperature, together with relevant literature data.

Complex	Photoproduct	$\tilde{\nu}$(CO)/cm^{-1}	λ_{max}/nm
[Re(Me)(CO)$_3$(*i*Pr-PyCa)]	product A	2001(s) 1889(s) 1874(s)	385
	product B	2019(s) 1917(s) 1889(m)	
[Re(Et)(CO)$_3$(*i*Pr-PyCa)]	product A	2002(s) 1888(s) 1872(s)	375
	product B	2021(s) 1918(s) 1891(m)	
[Re(Me)(CO)$_3$(*t*Bu-DAB)]	product A [a]	2001(s) 1884(s) 1862(s)	400
	product B	2019(s) 1914(s) 1890(s)	
[Re(Et)(CO)$_3$(*t*Bu-DAB)]	product A [a]	2001(s) 1883(s) 1860(s)	380
	product B	2020(s) 1911(s) 1890(s)	
[Re(Me)(CO)$_3$(*i*Pr-DAB)]	product A [a]	1998(s) 1880(s) 1863(s)	400
	product B	2021(s) 1912(s) 1888(s)	
[Re(Et)(CO)$_3$(*i*Pr-DAB)]	product A [a]	2000(s) 1882(s) 1867(s)	400
	product B	2017(s) 1909(s) 1890(s)	
[Re(Bz)(CO)$_3$(*i*Pr-DAB)]	product A [a]	2004(s) 1887(vs, br)	410
	product B	2021(s) 1912(s) 1888(s)	
[Re(THF)(CO)$_3$(*i*Pr-PyCa)]$^+$ [b]		2020(s) 1919(s) 1896(s)	380
[Re(THF)(CO)$_3$(*i*Pr-PyCa)]$^\bullet$ [b]		1995(s) 1875(s) 1851(s)	395
[Re(THF)(CO)$_3$(*i*Pr-DAB)]$^+$ [c]		2021(s) 1920(s) 1899(s)	
[Re(THF)(CO)$_3$(*i*Pr-DAB)]$^\bullet$ [c]		2007(s) 1891(s) 1875(s)	
[Re$_2$(CO)$_6$(C–C-*i*Pr-PyCa)$_2$] [b]		2014(s) 1993(s) 1907(m) 1890(vs) 1871(s)	390

[a] Only product at $T < 273$ K. [b] From ref. [34]. [c] From ref. [40].

  0947-6539/96/0202-0229 $ 10.00+.25/0

273 K, species A was the only product formed in the case of the [Re(R)(CO)$_3$(R'-DAB)] complexes. Raising the temperature after the irradiation led to the conversion of product A into product B. This shows that product A is the only photoproduct, which is thermally unstable and converts to product B at $T > 273$ K.

UV/Vis spectra measured in situ during the irradiation in THF at 273 K showed that the MLCT absorption band of the parent complex disappears and that a new, weaker band grows in at about 380 nm (Table 1). The spectral changes show an isosbestic point that remains well-defined until a rather large degree of conversion is reached. Formation of dimers [Re$_2$(CO)$_6$(α-diimine)$_2$], which was reported to occur after irradiation of [Re(R)(CO)$_3$(bpy)],[26] can thus be excluded here, since no absorption bands in the red spectral region, characteristic for this type of dimer,[12, 13, 34] were observed. Radical coupling leading to CC-coupled products can also be excluded since the IR frequencies of the CC-coupled dimer (Table 1)[34] do not correspond to those of any of the products formed.

Based on the spectroscopic data for the cations [Re(THF)(CO)$_3$(α-diimine)]$^+$ and the radicals [Re(THF)(CO)$_3$(α-diimine)]$^\bullet$ (Table 1), we tentatively assign A to a radical product and B to a cationic product. Up to now, all attempts to isolate the photoproducts have failed so no further characterization and confirmation of the assignment of the products was possible.

In order to demonstrate that the splitting of the Re–R bond observed in chlorinated solvents also occurs in THF, the [Re(R)(CO)$_3$(α-diimine)] complexes were photolysed in THF in the presence of a small excess of the spin trap nitrosodurene or *t*BuNO.[35–38] The photolysis was carried out in situ within the EPR spectrometer with 450 nm light selected from the output of a high-pressure mercury lamp by an interference filter. Formation of the radical adducts of both the [Re(CO)$_3$(α-diimine)]$^\bullet$ and R$^\bullet$ radicals with the spin traps was observed. The EPR results (coupling constants) are summarized in Table 2, while Figure 2 shows representative EPR spectra of trapped Et$^\bullet$ and [Re(CO)$_3$(*t*Bu-DAB)]$^\bullet$ radicals.

Table 2. EPR parameters [a] for the radical adducts R'N(O$^\bullet$)–Re(CO)$_3$(α-diimine) and R'N(O$^\bullet$)–R (R'NO = nitrosodurene (ArNO) or *t*BuNO) formed upon irradiation of [Re(R)(CO)$_3$(α-diimine)] with ArNO and *t*BuNO in THF (273 K).

Complex	ArNO–Re [b]	ArNO–R [b]	*t*BuNO–Re [c]	*t*BuNO–R [c]
*t*Bu-DAB/Me	n.o. [d]	$a_N = 14.0$	$a_N = 14.2$	$a_N = 16.5$
		$a_H = 12.5$	$a_{Re} = 35.9$	$a_H = 11.6$
*t*Bu-DAB/Et	n.o.	$a_N = 14.0$	$a_N = 14.2$	$a_N = 15.7$
		$a_H = 10.9$	$a_{Re} = 35.9$	$a_H = 10.6$
*i*Pr-DAB/Bz	n.o.	$a_N = 14.0$	$a_N = 14.1$	$a_N = 15.7$
		$a_H = 7.7$	$a_{Re} = 35.9$	$a_H = 7.0$
*i*Pr-PyCa/Me	$a_N = 14.0$ [e]	$a_N = 14.0$	$a_N = 14.5$	$a_N = 16.1$
	$a_{Re} = 36.1$	$a_H = 12.7$	$a_{Re} = 31.6$	$a_H = 11.9$
*i*Pr-PyCa/Et	$a_N = 14.05$ [e]	$a_N = 14.0$	$a_N = 14.5$	$a_N = 15.8$
	$a_{Re} = 36.1$	$a_H = 10.8$	$a_{Re} = 31.6$	$a_H = 10.4$

[a] Coupling constants in Gauss (±0.1). [b] Spin-adduct formed with 5-fold excess of nitrosodurene (ArNO). [c] Spin-adduct formed with 3-fold excess of *t*BuNO. [d] n.o. = Not observed. [e] Very low concentration.

The values of the EPR parameters of the trapped radicals agree reasonably well with previously reported values;[35, 38, 39] the small differences can be attributed to solvent effects (THF instead of benzene). It is clear that changing the ligand from R'-DAB to *i*Pr-PyCa causes a decrease in a_{Re} of the adducts, reflecting the stronger σ-donating and weaker π-accepting capacity of *i*Pr-PyCa. The total electron density is then higher at the metal atom and the electron becomes more localized at the oxygen atom of the spin trap. The data in Table 2 show that the spin traps have different selectivities for the [Re(CO)$_3$(α-diimine)]$^\bullet$ radicals. Thus, [Re(CO)$_3$(R'-DAB)]$^\bullet$ was trapped by *t*BuNO, whereas no radical adduct was detected in the presence of nitrosodurene. This phenomenon has been observed before[25] when a solution of [Ru(I)(*i*Pr)(CO)$_2$(*i*Pr-DAB)] was irradiated in the presence of either nitrosodurene (only trapped *i*Pr$^\bullet$ observed) or *t*BuNO (radical adducts with both *i*Pr$^\bullet$ and [Ru(I)(CO)$_2$(*i*Pr-DAB)]$^\bullet$ detected).

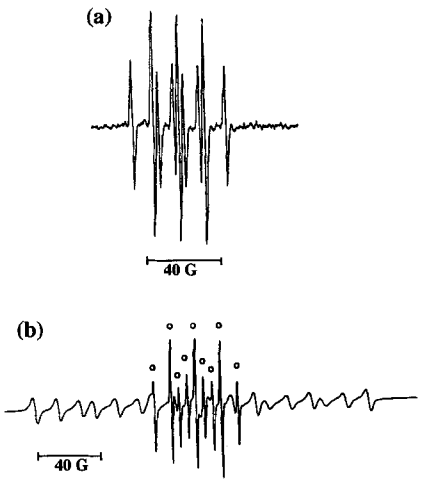

Fig. 2. EPR spectra of the radical adducts formed by the irradiation of [Re(Et)(CO)$_3$(*t*Bu-DAB)] in THF at 273 K in the presence of the spin traps nitrosodurene C$_6$H(CH$_3$)$_4$NO (a) and *t*BuNO (b). a) C$_6$H(CH$_3$)$_4$N(O$^\bullet$)–Et. b) *t*BuN(O$^\bullet$)–Et (indicated with o) together with *t*BuN(O$^\bullet$)–Re(CO)$_3$(*t*Bu-DAB).

In conclusion, the EPR spin-trapping experiments clearly show that the homolysis of the Re–R bond [Eq. (1)] is the primary photochemical reaction of [Re(R)(CO)$_3$(α-diimine)] complexes. The complicated follow-up thermal reactivity of the [Re(CO)$_3$(α-diimine)]$^\bullet$ radicals was not further investigated.

Quantum Yields: The efficiencies of the photoreactions of the complexes [Re(R)(CO)$_3$(α-diimine)] were determined by the measurement of the quantum yields (Φ) of their disappearance as a function of the irradiation wavelength, the temperature and, in some cases, the solvent. The quantum yield values obtained in THF are summarized in Table 3. Because of the thermal instability of [Re(Et)(CO)$_3$(*i*Pr-DAB)] at room temperature, all data were collected at 273 K. For the methyl complexes, the excitation wavelength dependences are presented in Figure 3, together with the absorption spectra.

As can be seen from Figure 3 and Table 3, the quantum yields show a remarkable dependence on the alkyl group. For R = Me, the quantum yield values are low (ranging from 0.033 for α-diimine = *i*Pr-DAB to 0.121 for *i*Pr-PyCa) and excitation-

Table 3. Quantum yields [a] of the photochemical homolysis of [Re(R)(CO)$_3$(α-diimine)] as a function of the excitation wavelength measured in THF.

	*i*Pr-PyCa		*t*Bu-DAB		*i*Pr-DAB		
λ/nm	Me × 10^1	Et	Me × 10^2	Et	Me × 10^2	Et	Bz
457.9	1.21	1.15	2.47	0.98	3.28	0.97	0.82
476.9	–	–	1.70	–	2.09	–	–
488.0	1.15	1.11	1.17	0.96	1.60	0.98	0.77
501.7	–	–	0.86	–	1.31	1.06	–
514.5	1.11	1.23	0.63	0.99	1.00	0.99	0.76

[a] $T = 273.0 \pm 0.1$ K; estimated error 5%.

0947-6539/96/0202-0230 $ 10.00+.25/0 Chem. Eur. J. 1996, 2, No. 2

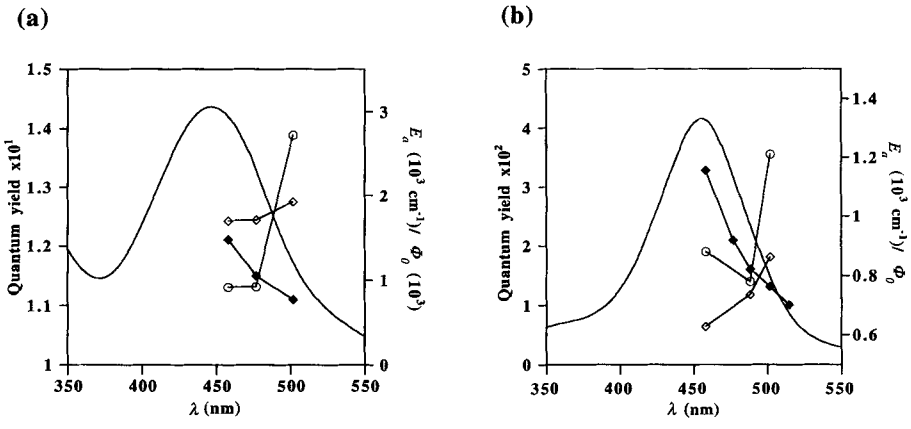

Fig. 3. Dependence of the quantum yields, activation energies and preexponential factors of the photochemical Re–Me homolysis of [Re(Me)(CO)$_3$(*i*Pr-PyCa)] (a) and [Re(Me)(CO)$_3$(*i*Pr-DAB)] (b) on the excitation wavelength in THF at 273 K. (◆ = Φ, ○ = Φ_0, ◇ = E_a).

wavelength dependent. Increasing the excitation energy results in a concomitant rise of the quantum yield. On the other hand, virtually no excitation wavelength dependence was found for R = Bz and Et. The quantum yields of these complexes are much larger, about 0.75 for R = Bz and 1 or even slightly higher for [Re(Et)(CO)$_3$(*i*Pr-PyCa)]. In the latter case, the Et radical seems to react also with the starting material.

Apart from a dependence on the alkyl group, the quantum yield also depends on the α-diimine used. The quantum yield of [Re(Me)(CO)$_3$(α-diimine)] increases from *i*Pr-DAB to *i*Pr-PyCa by a factor of about four. For α-diimine = bpy, a quantum yield value of 1 has even been reported.[26]

The temperature dependence of the quantum yield of the [Re(R)(CO)$_3$(α-diimine)] complexes was investigated by the measurement of the quantum yields at 4 different temperatures at several excitation wavelengths. In this case too a dependence on the alkyl group was found. No significant temperature dependence was seen for the efficient homolysis reactions of the Et and Bz complexes, whereas the Me complexes showed a considerable decrease in quantum yield with decreasing temperature. The experimental values for [Re(Me)(CO)$_3$(α-diimine)] can be fitted to an Arrhenius-type equation: $\Phi = \Phi_0 \exp(-E_a/RT)$ with high correlation coefficients (> 0.995). The calculated activation energies E_a and preexponential factors Φ_0 are collected in Table 4, while Figure 3 shows their dependence on the excitation wavelength.

Table 4. Quantum yields (× 10^2) [a] and activation parameters (E_a, Φ_0) of the photochemical homolysis of [Re(Me)(CO)$_3$(α-diimine)] as a function of the irradiation wavelength measured in THF (253 < *T* < 283 K) (*T* in K, λ_{exc} in nm, E_a in cm^{-1}).

	*i*Pr-PyCa			*t*Bu-DAB		*i*Pr-DAB		
	457.9	476.9	501.7	457.9	488.0	457.9	488.0	501.7
283	15.9	15.6	15.7	2.73	1.45	3.45	1.85	1.52
273	12.1	11.5	11.1	2.47	1.17	3.28	1.60	1.31
263	8.15	8.11	7.45	1.85	0.96	2.77	1.40	1.07
253	5.81	5.59	4.96	1.46	0.86	2.46	1.18	0.91
E_a	1697	1705	1923	1078	878	627	736	861
Φ_0	915	920	2720	6.9	1.2	0.9	0.8	1.2

[a] *T* ± 0.1 K; estimated error 5%.

For [Re(Me)(CO)$_3$(*t*Bu-DAB)], Φ was measured in THF, 2-MeTHF and toluene (λ_{exc} = 488 nm, *T* = 273 K), the values being 0.0117, 0.0117 and 0.0103, respectively. The solvent influence on the quantum yield of [Re(Bz)(CO)$_3$(*i*Pr-DAB)] was studied in more detail and the results are collected in Table 5. It clearly follows that the quantum yield is, within experimental error, identical in THF and in toluene.

Table 5. Solvent and temperature dependence of the quantum yield [a] of the photochemical homolysis of [Re(Bz)(CO)$_3$(*i*Pr-DAB)].

λ_{exc}/nm	THF, 273 K	THF, 253 K	toluene, 273 K	toluene, 253 K
457.9	0.82	0.79	0.75	0.79
488.0	0.77	0.75	0.77	0.73
514.5	0.76	0.71	0.72	0.72

[a] *T* = 273.0 ± 0.1 K; estimated error 5%.

Time-Resolved Spectroscopy: In order to gain more insight into the excited-state dynamics and nature of the intermediates involved in the photochemistry of the [Re(R)(CO)$_3$(α-diimine)] complexes, a flash photolysis study with UV/Vis absorption detection was carried out in the ps–μs time domain, while the IR spectra were studied in the ns–μs range. To obtain the ns–μs UV/Vis spectra, solutions of the complexes were excited either at 532 nm or 460 nm, depending on the ground-state absorption maximum, and the transient absorption spectra were taken at different time delays after the laser pulse. Picosecond spectra could only be obtained with 532 or 355 nm, which somewhat limited the choice of the complexes. The solvent dependence of the transients was investigated by comparing the spectra obtained in THF and in toluene for all complexes studied. A more detailed solvent dependence study was carried out for [Re(Bz)(CO)$_3$(*i*Pr-DAB)], in which cyclohexane, benzene, 2-MeTHF, 2-chlorobutane and CH_3CN were also used. Generally, two basic types of excited-state behaviour were observed: one for the relatively photostable methyl complexes and another for their highly reactive ethyl and benzyl congeners. Picosecond absorption spectra of [Re(Me)(CO)$_3$(*t*Bu-DAB)] and [Re(Me)(CO)$_3$(*p*An-DAB)] (see Figs. 4a and b) show considerable bleaching of the ground-state absorption together with a weak transient absorption at longer wavelengths that extends over the whole visible spectral region, overlapping partly with the bleached ground-state absorption. In accordance with the ps time-resolved spectrum of [Re(Br)(CO)$_3$(*p*Tol-DAB)],[40] it is assigned to the Re → R′-DAB MLCT excited state, the intensity of the excited-state absorption being lower for the complexes of the DAB ligands bearing aliphatic substituents (*t*Bu, *i*Pr). Both the bleach and transient absorption are fully developed within the 30 ps excitation laser pulse. For [Re(Me)(CO)$_3$(*t*Bu-DAB)], the intensities of both the bleach and the transient absorption decay by about 50% within 500 ps after the excitation, indicating that the excited state deactivation is dominated by a rather fast nonradiative transition to the ground state. The picosecond absorption spectrum of [Re(Me)(CO)$_3$(*p*An-DAB)] shows absorptions caused by two transients. The short-lived one absorbs between 530 and 630 nm and

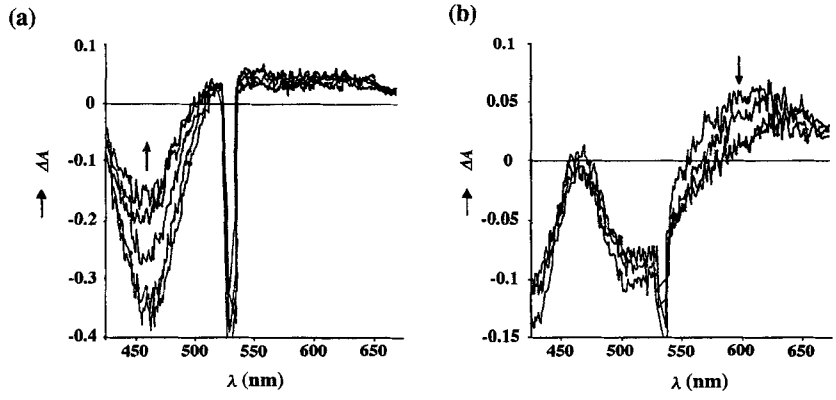

Fig. 4. Picosecond transient absorption spectra of [Re(Me)(CO)$_3$(R'-DAB)] complexes. a) [Re(Me)(CO)$_3$(*t*Bu-DAB)] in CH_2Cl_2 at 20, 50, 100, 200 and 500 ps following laser excitation at 532 nm in order of decreasing bleach. b) [Re(Me)(CO)$_3$(*p*An-DAB)] in CH_2Cl_2 at 20, 50, 200 ps and 1 ns following laser excitation at 532 nm in order of decreasing absorption at 600 nm. (Note that the difference absorption spectra are shown, the negative absorbance corresponding to the bleached ground-state absorption).

decays within 250 ps, leaving another transient absorbing weakly above 630 nm that persists over about 10 ns. By analogy with the complex [Re(Br)(CO)$_3$(*p*An-DAB)],[40] which exhibits very similar excited-state behaviour on the picosecond timescale, the short- and long-lived transients of [Re(Me)(CO)$_3$(*p*An-DAB)] are tentatively assigned to the MLCT and *p*An-DAB intraligand (IL) excited states, respectively.

In accordance with the results obtained in the picosecond time domain, almost no transient absorption was observed for any of the [Re(Me)(CO)$_3$(α-diimine)] complexes in THF or in toluene by nanosecond laser flash photolysis. This means that the excited states of all the methyl complexes studied have lives much shorter than 20 ns.

The time-resolved absorption spectra of all the photoreactive [Re(Et)(CO)$_3$(α-diimine)] and [Re(Bz)(CO)$_3$(α-diimine)] complexes demonstrate a common behaviour that will be explained by means of [Re(Bz)(CO)$_3$(*i*Pr-DAB)] as a representative example. The difference absorption spectrum (425–675 nm) obtained 50 ps after excitation of a THF solution of this complex at 532 nm shows only bleached ground-state absorption, the signal observed being just a mirror image of the ground-state absorption spectrum (see Fig. 5a). It does not change over the next 10 ns. In accord with this observation, the spectrum measured by nanosecond laser flash photolysis shows only one absorption band at 390 nm that is already fully developed within the 7 ns laser pulse and whose intensity remains constant over at least the next 15 μs. No ns transient absorption in the visible region was found (Fig. 6a). A markedly different behaviour was observed in toluene. The picosecond absorption spectrum taken 20 ps after the excitation pulse (Fig. 5b) clearly shows the presence of a transient whose strong absorption band at about 500 nm is superimposed over the negative bleached ground-state absorption. The absorption band at 500 nm is fully developed within the excitation pulse and it remains unchanged, both in intensity and position, over the next 10 ns. Accordingly, spectra measured by nanosecond laser flash photolysis (Fig. 6b) exhibit a transient absorption band at 500 nm that is already fully developed within the 7 ns excitation pulse and whose intensity decays according to single-exponential kinetics with a lifetime of about 250 ns. Concomitantly with the decay of the 500 nm transient, a product absorbing at 390 nm is formed according to the same kinetics. This product appears to be identical to that formed immediately in THF. Nanosecond absorption spectra measured in various solvents show that the transient species absorbing at about 500 nm is formed only in noncoordinating solvents and relatively nonpolar solvents such as toluene, benzene and cyclohexane. The absorption maxima and lifetimes are summarized in Table 6. In contrast, prompt formation of the final product absorbing at 380–390 nm was observed in the coordinating and/or polar solvents THF, 2-MeTHF, CH_3CN and 2-chlorobutane.

Other [Re(Et)(CO)$_3$(α-diimine)] and [Re(Bz)(CO)$_3$(α-diimine)] complexes behave in essentially the same way as described above for

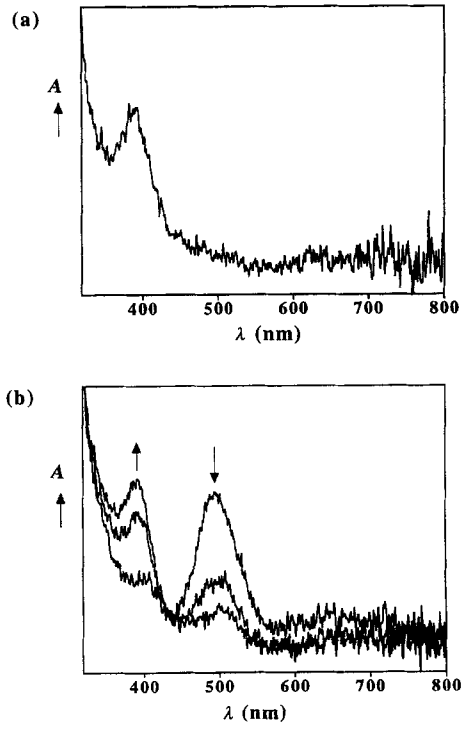

Fig. 6. Nanosecond transient absorption spectra of [Re(Bz)(CO)$_3$(*i*Pr-DAB)] in a) 2-MeTHF at 30 ns and b) toluene at 30 ns, 230 ns and 430 ns after the 532 nm excitation pulse. The spectra are corrected for the bleaching of the ground-state absorption of the parent compound.

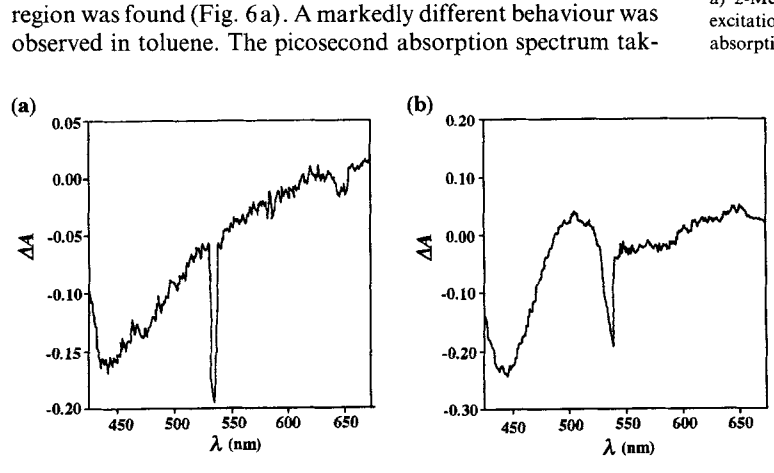

Fig. 5. Picosecond transient absorption spectra of [Re(Bz)(CO)$_3$(*i*Pr-DAB)] in a) THF and b) toluene at 50 ps after 532 nm excitation.

0947-6539/96/0202-0232 $ 10.00+.25/0 Chem. Eur. J. 1996, 2, No. 2

Table 6. Absorption maxima [a] and lifetimes [b] of transients formed after flash photolysis of [Re(R)(CO)$_3$(α-diimine)] (R = Bz, Et) in different solvents.

R/α-diimine	solvent	Transient 1 [c] λ_{max}	lifetime/ns	Transient 2 [d] λ_{max}
Et/*i*Pr-DAB	toluene	495	60	385
Bz/*i*Pr-DAB	toluene	500	250	390
	benzene	500	90	
	cyclohexane	495	155	
Et/*t*Bu-DAB	toluene	502	60	380
Bz/*t*Bu-DAB	toluene	510	275	380
Et/*i*Pr-PyCa	toluene	525	20	405

[a] Wavelength in nm (±5 nm). [b] Due to the relatively low absorptions the signal-to-noise ratio is not high enough for accurate determinations, so reported lifetimes are rough estimates (±10%). [c] Transient formed in noncoordinating solvents. [d] Transient formed immediately in THF and after decay of transient 1 in noncoordinating solvents; reported values in THF.

[Re(Bz)(CO)$_3$(*i*Pr-DAB)]. Results obtained are summarized in Table 6. There are only small variations in the position of the absorption band of the "500 nm" transient found for all these complexes in toluene. In all cases, this transient converts into the photoproduct absorbing around 380 nm. In THF, the same product is always formed much more rapidly, within the picosecond excitation laser pulse, without any observable intermediates. This photoproduct is stable for at least 15 μs, with the single exception of the photoproduct of [Re(Et)(CO)$_3$(*i*Pr-PyCa)] for which a further reaction was found that diminished its lifetime to about 2 μs. The [Re(Et)(CO)$_3$(*i*Pr-PyCa)] complex showed in addition a third broad transient absorption with an absorption maximum at about 600 nm. This transient had a very short lifetime (< 20 ns) and was seen in THF as well as in toluene. A similar weak absorption band was observed as the only transient for [Re(Me)(CO)$_3$(*i*Pr-PyCa)] in both solvents. By analogy with the transient absorption of [Re(Br)(CO)$_3$(*i*Pr-PyCa)] (λ_{max} = 560 nm, τ < 20 ns), it is assigned to the Re → *i*Pr-PyCa MLCT state.

Time-resolved infrared spectra of [Re(Bz)(CO)$_3$(*i*Pr-DAB)] in the region of the CO stretching vibrations, ν(CO), were measured[32] in order to get more structural information on the intermediate, that is, the "500 nm" transient, and on the product observed in the time-resolved UV/Vis absorption spectra. Shown in Figure 7a is the difference IR absorption spectrum of the [Re(Bz)(CO)$_3$(*i*Pr-DAB)] complex measured in a *n*-heptane solution 120 ns after excitation with a 10 ns 532 nm laser pulse. It shows negative peaks at 2009, 1916 and 1909 cm^{-1} caused by the depletion of the starting complex and the formation of a transient species with CO frequencies that are slightly shifted to about 2015 and 1909 (br) cm^{-1} (exact band frequencies could not be determined because of the overlap with the ground state and photoproduct spectra). In accord with the results obtained by UV/Vis time-resolved spectroscopy, this transient was found to decay with the concomitant formation of a product characterized by IR bands at approximately 2023 and 1900 (br) cm^{-1}. This is seen in Figure 7b, which shows the IR spectrum obtained 3.5 μs after the excitation. The conversion of the transient into the product occurs single-exponentially with a lifetime in the range 210–290 ns, in agreement with the results of the time-resolved UV/Vis spectra (the actual lifetimes measured depend slightly on the monitoring IR frequency because of the strong overlap of the IR bands involved). No concomitant recovery of the bleached ground-state absorption was observed. The formation of the transient and photoproduct was completely quenched by oxygen, indicating that the primarily observed transient can indeed be assigned to an excited state. By comparison with the IR spectra of [Re(S)(CO)$_3$(*i*Pr-DAB)]$^{\bullet}$ radicals[41] (2005 and 1894 (br) cm^{-1} for S = *n*PrCN, and 2007, 1891, 1877 cm^{-1} for S = THF), the IR spectrum of the photoproduct is assigned to the [Re(CO)$_3$(*i*Pr-DAB)]$^{\bullet}$ radical. The small positive shift of the ν(CO) frequencies is expected because of the absence of an electron-donating coordinated solvent molecule and because of a general solvent effect found even for [Re(Bz)(CO)$_3$(*i*Pr-DAB)] itself (– 9 cm^{-1} going from *n*-heptane to THF). Apart from this radical, formation of another product absorbing weakly at about 1992 cm^{-1} occurs directly from the initial transient, as shown by the kinetic traces measured at this frequency. It may correspond either to some unidentified byproduct or to an isomeric form of the pentacoordinated radical. The time-resolved IR spectrum obtained in CH_3CN in the region of the high frequency ν(CO) band showed only bleached ground-state absorption and a photoproduct band at slightly higher frequency which appears as soon as 120 ns after the laser pulse and which decays in intensity by 25% over the next 50 μs. No evidence for any intermediate species was found in the CH_3CN solution. The broadness of the IR bands observed in CH_3CN prevented a more detailed study.

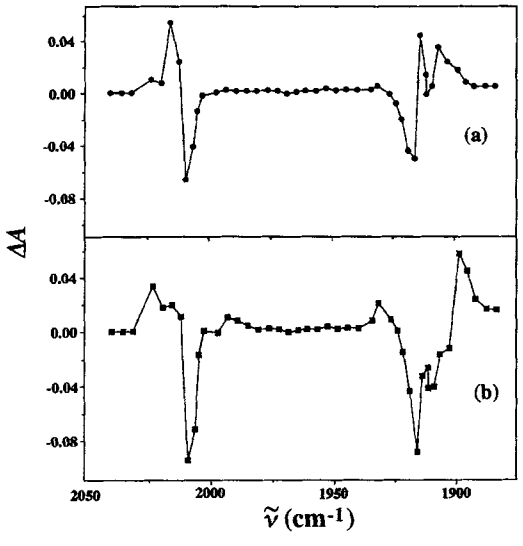

Fig. 7. Time-resolved infrared spectra of [Re(Bz)(CO)$_3$(*i*Pr-DAB)] in *n*-heptane at 293 K. a) TRIR spectrum at 120 ns after the laser flash (532 nm, 10 ns); b) TRIR spectrum at 3.5 μs after the laser flash.

Discussion

The experimental results discussed above clearly show that the homolytic splitting of the Re–R bond [Eq. (1)] is the primary photochemical step for all the [Re(R)(CO)$_3$(α-diimine)] complexes studied. The ultimate fate of the photochemically produced radicals depends on the solvent used: they abstract chlorine or hydrogen atoms, dimerize, decompose or disproportionate.

Photochemical homolysis of a metal–ligand bond upon MLCT excitation is a process characteristic of those complexes that contain in their coordination sphere a σ-bonded ligand with a high-lying σ-orbital (e.g., metal-containing groups, alkyls) and an electron-accepting ligand with an unoccupied, energetically accessible π* orbital, usually, but not necessarily, an α-diimine ligand. Complexes like [L_nM–Re(CO)$_3$(α-diimine)] (L_nM = Ph_3Sn,[15] $(CO)_5Re$,[2, 11, 12, 42] $(CO)_2$(Cp)Fe[43]), [$(CO)_5$MnRu(Me)$(CO)_2$(*i*Pr-DAB)][19] as well as molecules containing metal–alkyl bonds like [Re(R)(CO)$_3$(bpy)],[26] [Mn(R)(CO)$_3$(R'-DAB)][27] and [Ru(I)(*i*Pr)$(CO)_2$(*i*Pr-DAB)][25]

may serve as typical examples. Analogous behaviour has been observed for the non-carbonyl complexes $[Pt(Me)_4(\alpha\text{-diimine})]$[21,22] and $[Zn(Me)_2(R'\text{-DAB})]$,[20] as well as for $[Ir(R)(CO)(PAr_3)_2(mnt)]$[23] (mnt = maleonitriledithiolate) and for $[Ir\{(6\text{-isopropyl-8-quinolyl})diorganosilyl\}_3]$ (diorgano = Me_2, Ph_2 or PhMe)[44-46] complexes. For the latter two types of complexes, the mnt ligand and the *N*-coordinated quinolyl group serve as the π^* electron-accepting sites. Recent interpretation of the photoreactivity of all these complexes assumes[1,47] the involvement of a reactive $\sigma\pi^*$ excited state originating in electron excitation from the σ bond to be split to the π^* orbital of the acceptor ligand (α-diimine). However, direct characterization of these $\sigma\pi^*$ excited states has so far proved rather elusive. Only in the case of the $[Ir\{(6\text{-isopropyl-8-quinolyl})diorganosilyl)\}_3]$ complexes a strong solvent-dependent emission was found,[45] presumably from the $\sigma(Ir-Si)\pi^*$ excited state, together with the absorption spectrum of the $\sigma\pi^*$ state dominated by the bands of the reduced quinolyl group.[46] The lifetime of the $\sigma(Ir-Si)\pi^*$ state was found to be much shorter in coordinating solvents than in hydrocarbons.

The $[Re(R)(CO)_3(\alpha\text{-diimine})]$ complexes under study are typical representatives of this family of photoreactive compounds. Significant population of the $\sigma(Re-R)\pi^*$ excited state is expected for the strongly photoreactive species with R = Et or Bz. Indeed, all the ethyl and benzyl complexes show the prompt formation of a transient species that absorbs at about 500 nm, from which the radicals are produced. Hence we propose that this transient represents the complex in its $\sigma\pi^*$ excited state. The 500 nm excited-state absorption is tentatively assigned to the $d_\pi \rightarrow \sigma$ excitation, that is, to a transition from the $\sigma\pi^*$ excited state to a higher-lying MLCT state. The assignment of the "500 nm" transient to the $\sigma\pi^*$ excited state is further supported by the detailed TRIR study.[32] The electron density on the Re atom is expected to be rather similar in the ground and $\sigma\pi^*$ electronic states as the $\sigma \rightarrow \pi^*$ excitation does not directly affect the population of the d_π orbitals and the diminished electron donation from R is offset by the decreased π back-donation to and increased σ-donation from the α-diimine ligand. Accordingly, only a very small shift of the CO stretching frequencies from the ground-state values was found in the IR spectrum of the transient generated from $[Re(Bz)(CO)_3(i\text{Pr-DAB})]$ (Fig. 7a). This shows that the extent of the $Re \rightarrow CO\,\pi$ back-donation is virtually the same as in the ground state, lending further support for the assignment of the "500 nm" transient to the $\sigma\pi^*$ state.

Interestingly, the relatively long lifetime (250 ns) of the $\sigma\pi^*$ excited state of the $[Re(R)(CO)_3(\alpha\text{-diimine})]$ (R = Et, Bz) complexes and the well-developed excited-state visible and IR absorption bands indicate that this state is not inherently dissociative, despite the depopulation of the $\sigma(Re-R)$ bonding orbital. The potential energy surface of the $\sigma\pi^*$ state appears to have a well-defined energetic minimum, from which the Re–R bond dissociation takes place with unit efficiency ($k = 4 \times 10^6\ s^{-1}$ in toluene), the nonradiative return to the ground state (if any) being much slower and kinetically completely uncompetitive. This conclusion is supported by the time-resolved experiments, which showed that no ground-state regeneration occurs at all during the decay of the $\sigma\pi^*$ state. The surprising stability of the $\sigma\pi^*$ state towards the unproductive deactivation to the ground state may be explained by assuming it has spin-triplet "biradical" character, $[R^{\bullet}-Re^{I}(CO)_3(\alpha\text{-diimine}^{\bullet-})]$. A small distortion of the $\sigma\pi^*$ state with respect to the ground state, found for emissive $[(CO)_5MnRu(Me)(CO)_2(\alpha\text{-diimine})]$ complexes,[29] might also contribute to the long, nonreactive, lifetime of the $\sigma\pi^*$ state.

The lifetime of the $\sigma\pi^*$ excited state decreases dramatically in coordinating solvents like THF, where the radical product formation is fully completed within 30 ps. A similar, albeit less pronounced, solvent-dependent drop in the $\sigma\pi^*$ lifetime was found for the Ir–silyl complexes.[44-46] Apparently, the interaction between the Lewis basic solvent molecule and the electron-deficient Re–Bz one-electron bond in the $\sigma\pi^*$ excited state modifies the potential energy surface of the $\sigma\pi^*$ excited state to such an extent that the reacting system smoothly evolves into the reaction products.

Our previous spectroscopic study of the $[Re(R)(CO)_3(\alpha\text{-diimine})]$ complexes[31] showed that their visible absorption bands, into which the excitation occurred during the photochemical experiments, correspond to $Re \rightarrow \alpha$-diimine MLCT transitions. Hence, the first step involved in the excited-state dynamics, one that is ultimately responsible for the Re–R bond homolysis, has to be the MLCT $\rightarrow \sigma\pi^*$ conversion that involves a symmetry- and overlap-allowed transfer of an electron from the σ to the d_π orbital. The picosecond absorption spectra show that this conversion into the, presumably spin-triplet, $\sigma\pi^*$ excited state is very rapid, being fully completed within the 30 ps excitation pulse in both THF and toluene; this indicates a subpicosecond rate for the process. This conclusion agrees with the large quantum yield values found for the photolysis of the ethyl and benzyl complexes. Remarkably, identical quantum yields (≈ 0.75, see Table 5) were measured for $[Re(Bz)(CO)_3(i\text{Pr-DAB})]$ in toluene and THF despite completely different timescales for the Re–Bz homolysis, hundreds of nanoseconds versus subpicosecond, respectively. This, together with the absence of any $\sigma\pi^*$ deactivation to the ground state, indicates that the overall photochemical quantum yield is determined by the efficiency of the MLCT $\rightarrow {}^3\sigma\pi^*$ conversion that is about 0.75, independent of the solvent used. Moreover, the independence of the quantum yields on the excitation energy and temperature, together with the prompt nature of the MLCT $\rightarrow \sigma\pi^*$ conversion, indicate that the $\sigma\pi^*$ state lies lower in energy than the MLCT state, their potential energy surfaces crossing each other close to the energetic minimum of the MLCT state.

Compared with those of the ethyl and benzyl complexes, the quantum yields from the homolytic splitting of the Re–Me bond in the $[Re(Me)(CO)_3(\alpha\text{-diimine})]$ complexes studied are much lower and excitation wavelength- and temperature-dependent. Assuming that the $\sigma\pi^*$ excited state of the methyl complexes is as reactive as in their ethyl and benzyl analogues, the different photochemical behaviour of the methyl complexes seems to be caused by a different mechanism of the population of the reactive $\sigma\pi^*$ state. The UV-PE spectra of the $[Re(Me)(CO)_3(i\text{Pr-DAB})]$ and $[Re(Me)(CO)_3(i\text{Pr-PyCa})]$ complexes show that the ionization potential of the σ electron is higher by about 1 eV than the average ionization potential of the d_π electrons.[31] It therefore appears that the σ orbital lies well below the d_π orbitals, thus placing the reactive $\sigma\pi^*$ excited state at higher energy than the optically populated $d_\pi\pi^*$ MLCT excited states (Fig. 8). The temperature dependence of the quantum yields indeed shows that extra energy is needed to populate the $\sigma\pi^*$ state after the MLCT excitation. Moreover, the quantum yield increases with increasing excitation energy, and the activation energy decreases concomitantly (Fig. 3). These results clearly show that the crossing between the MLCT and $\sigma\pi^*$ potential energy surfaces in the relatively unreactive methyl complexes takes place at energies well above the minimum of the MLCT state. Hence, the MLCT $\rightarrow \sigma\pi^*$ conversion is promoted by high-energy excitation into higher vibronic levels of the MLCT state. In fact, the dependence of the quantum yields of the homolytic Re–Me bond-splitting on excitation energy and

0947-6539/96/0202-0234 $ 10.00+.25/0 Chem. Eur. J. 1996, 2, No. 2

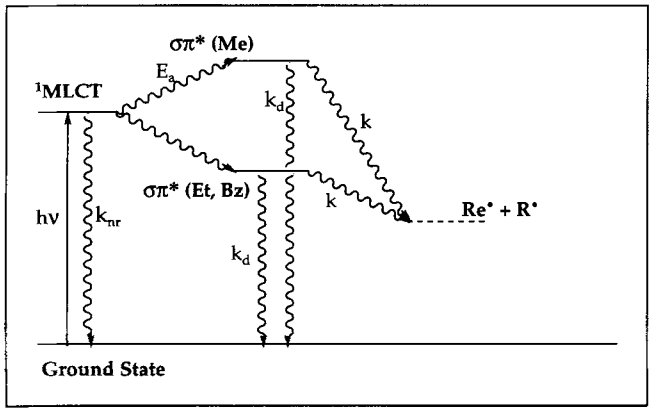

Fig. 8. Excited-state dynamics of the [Re(R)(CO)$_3$(α-diimine)] complexes. For R = Me, the conversion from the MLCT to the σπ* excited state is an activated process, E_a. The reactive σπ* excited state can be depopulated by a reactive (k) or a deactivation pathway (k_d), the former dominating.

temperature closely resembles that of the quantum yield of CO dissociation from the MLCT-excited [Cr(CO)$_4$(bpy)] complex.[48, 49] It is quite possible that the reactivity of the [Re(Me)(CO)$_3$(α-diimine)] complexes may be interpreted with a similar model[49] in which the MLCT excited state is vibronically coupled with the σπ* state along the reaction coordinate. The energy barrier would then arise from an avoided crossing between these two excited states.

Finally, it should be noted that the coupled dependence of the quantum yields of the Re–Me bond homolysis on excitation energy and temperature excludes an alternative interpretation of the activation energy observed as originating from the energy barrier of the dissociation of the stable Re–Me bond from the σπ* state. If this were the case, the quantum yield would have been temperature-dependent but independent of the excitation energy, as all the memory of the original Franck–Condon excitation would have been lost during the conversion to the σπ* state and its thermalization. Moreover, a build-up of a substantial concentration of σπ*-excited molecules, which was not observed spectroscopically, would have been expected.

Going from the [Re(Me)(CO)$_3$(R′-DAB)] complexes to [Re(Me)(CO)$_3$(*i*Pr-PyCa)] the activation energy increases, on the average, by almost 1000 cm^{-1}. However, the photochemical quantum yield concomitantly increases about 5-fold because of a large increase of the preexponential factor Φ_0 apparently caused by a decrease in the rate of a competitive unproductive deactivation of the MLCT state by its nonradiative transition to the ground state, k_{nr}.[50] Such a pronounced decrease in the rate constant of the nonradiative deactivation of the MLCT state on changing from DAB to PyCa has been observed in many α-diimine complexes. For example, the corresponding values calculated from the emission data measured at 80 K for [Re(Br)(CO)$_3$(α-diimine)] decrease from 1.7×10^7 to 1.4×10^6 s^{-1} when the ligand is changed from *i*Pr-DAB to *i*Pr-PyCa, supporting the above conclusion.

The above discussion of the mechanism of the Re–R bond homolysis in [Re(R)(CO)$_3$(α-diimine)] complexes points to the critical role played by the relative energetic positions of the optically populated MLCT and the reactive σπ* states, which are controlled by the nature of the alkyl ligand. Hence, the strongly donating methyl ligand gives rise to a relatively stable σ(Re–Me) bonding orbital that lies well below the d_π orbitals, as was proved by the UV-PE spectra. Weaker bonding and electron donation from the ethyl and, especially, benzyl ligands apparently leads to a reversal of the MLCT and σπ* excited states, the latter becoming the lowest-lying excited state, which may thus be easily and efficiently populated from the optically excited MLCT states. The influence of the alkyl ligand on the excited states of the [Re(R)(CO)$_3$(α-diimine)] complexes is shown in Figure 8. Unfortunately, it was not possible to demonstrate the low-energy shift of the σ(Re–R) orbital upon changing the R ligand from Me to Et and to Bz by UV-PE spectroscopy since the ethyl and methyl complexes do not have sufficient vapour pressure to obtain these spectra. However, it should be noted that the essential features, that is, large, temperature- and excitation wavelength-independent quantum yields of the Re–R bond homolysis in the highly photoreactive [Re(Et)(CO)$_3$(α-diimine)] and [Re(Bz)(CO)$_3$(α-diimine)] complexes were found also for the metal–metal bond homolysis in [L$_n$M–Re(CO)$_3$(α-diimine)] complexes whose UV-PE spectra clearly demonstrate that the σ(M–Re) orbital lies above the d_π(Re) orbitals.[51] Moreover, spectra and MO calculations of [ZnR$_2$(R′-DAB)] complexes showed[20] that the σ(Zn–R) orbital energy decreases significantly when R is changed from Et to Me. This effect was explained by a hyperconjugative destabilization of the σ lone electron pair in the (formally) carbanionic Et ligand[20] and it may well be expected to occur also for the Re–R bond. Also a hyperconjugative interaction with the C–H bonding orbitals of the Me ligand would destabilize the d_π orbital in [Re(Me)(CO)$_3$(α-diimine)]. Both these effects may contribute to the reversal of the energetic order of the σ(Re–R) and d_π orbitals and, hence, of the σπ* and MLCT excited states in the [Re(Me)(CO)$_3$(α-diimine)] complexes as compared with their Et analogues, accounting thus for the remarkable change in photoreactivity.

Conclusions

Irradiation of [Re(R)(CO)$_3$(α-diimine)] complexes (R = Me, Et, Bz; α-diimine = *i*Pr-PyCa, R′-DAB) into their visible MLCT absorption band results in a homolytic splitting of the Re–R bond, which occurs as a primary photochemical step. This reaction takes place via a σπ* excited state from which the radical products are formed without any further intermediates. Dissociation of the Re–R bond in the σπ* state is strongly accelerated by donor or polar solvents. Despite significant weakening of the Re–R bond, the σπ* state is, at least in noncoordinating solvents, rather long-lived (250 ns). It is a bound state with a well-defined energetic minimum and, hence, equilibrium geometry. It is spectroscopically characterized by a, presumably σπ* → MLCT, transition at about 500 nm and by CO stretching frequencies close to their ground-state values, implying only a very small change in the electron density on the Re atom upon the σ → π* excitation.

Population of the optically inaccessible σπ* state by a nonradiative transition from the optically populated MLCT state is fast (subpicosecond) and very efficient as long as the σπ* state lies at lower energy than the MLCT state. The intense MLCT spectral transition provides an efficient gateway for the energy that is then channelled to the σπ* state and utilized chemically in the Re–R bond splitting. The σπ* state may be populated, albeit less efficiently, even if it lies above the MLCT state through an activated process that appears to involve vibronic coupling between the σπ* state and MLCT excited states.

The [Re(R)(CO)$_3$(α-diimine)] complexes studied closely in this paper represent the whole family of the photodissociative alkyl- and metal–metal bonded organometallics containing an electron-accepting α-diimine ligand. Hence, the conclusions on the involvement of the σπ* state in the photochemical bond

homolysis, on its properties and on the determining role of the mechanism of its population have rather general implications. Further investigation of the properties and reactivity of the $\sigma\pi^*$ excited state are continuing in our laboratories.

Experimental Section

Materials and Preparation: The synthesis of the ligands R'-DAB and *i*Pr-PyCa and of the complexes $[Re(R)(CO)_3(R'\text{-DAB})]$ (R = Me, Et, Bz; R' = *i*Pr, *t*Bu, *p*An) and $[Re(R)(CO)_3(i\text{Pr-PyCa})]$ (R = Me, Et) has been described elsewhere [31,52]. The complexes were identified by FTIR, UV/Vis, ^{1}H NMR and mass spectroscopy. The spin traps 2,3,5,6-tetramethylnitrosobenzene (nitrosodurene) and 2-methyl-2-nitrosopropane dimer (*t*BuNO, Aldrich) were commercially obtained and used without further purification. Solvents for spectroscopy and for photochemical experiments were of analytical grade (THF, 2-MeTHF, toluene, hexane, 2-chlorobutane, CH_2Cl_2, CH_3CN) or Uvasol (cyclohexane), dried over sodium (THF, hexane, toluene, 2-MeTHF), $CaCl_2$ (2-chlorobutane, CH_2Cl_2), CaH_2 (CH_3CN) or molecular sieves (cyclohexane) and distilled under N_2 prior to use.

Spectroscopic Measurements and Photochemistry: All preparations for photochemical experiments were carried out under an atmosphere of purified N_2 using Schlenk techniques. The solutions were stored and handled in darkness before the experiments were performed. For the photochemical conversions the complexes were irradiated either with one of the lines of an SP 2025 Argon ion laser or with a Philips HPK 125 W high pressure Hg lamp equipped with an appropriate interference filter. Electronic absorption spectra were measured on a Varian Cary 4 E spectrophotometer or a Perkin–Elmer Lambda 5 UV/Vis spectrophotometer, the latter provided with a 3600 Data Station. Infrared spectra were recorded with either a Biorad FTS-7 FTIR spectrometer or a Biorad FTS-60 A FTIR spectrometer equipped with a liquid-nitrogen-cooled MCT detector. An Oxford Instruments DN 1704/54 liquid nitrogen cryostat was used for low-temperature IR and UV/Vis measurements. ^{1}H NMR spectra were recorded on a Bruker AMX 300 spectrometer. To measure ^{1}H NMR spectra of in situ photolysed solutions the spectrometer was equipped with a special Bruker CIDNP 300 MHz ^{1}H probe. The sample was irradiated through a glass fibre (d = 8 mm) by a water-cooled Oriel AG 150 mW high-pressure lamp with suitable cut-off filters. Concentrations varied between 10^{-4}–10^{-3} M. EPR spectra were recorded on a Varian E6 EPR spectrometer equipped with a temperature controller. Typical sample concentrations for these measurements were 5×10^{-3} M. Laser flash photolysis was used to obtain the ps and ns transient absorption spectra. Nanosecond absorption spectra in the visible spectral region were measured after the excitation of the sample with 7 ns (fwhm) pulses of a Spectra Physics GCR-3 Nd:YAG laser. The desired excitation wavelength was obtained by frequency doubling of the 1064 nm 10 Hz fundamental (532 nm), or by means of a Quanta-Ray PDL-3 pulsed dye laser (Spectra Physics) with a suitable dye (Coumarin 47 for λ_{exc} = 460 nm) pumped with the third harmonic frequency of the Nd:YAG laser. Typical pulse energies were 20 mJ per pulse for 532 nm and 14 mJ per pulse for 460 nm excitation. The sample absorbance at the excitation wavelength was kept between 0.3 and 0.9 and the maximum absorbance did not exceed 1.2. A 450 W high-pressure Xe lamp pulsed with a Müller Elektronik MSP05 pulser was used as a probe source. After passing through the sample, the probe light was transferred through an optical fibre to a spectrograph (EG & G Model 1234) equipped with a 150 g mm^{-1} grating and a 250 μm slit resulting in a 6 nm resolution. The data collection system consisted of a Model 1460 OMA-III console provided with a 1302 fast pulser, a 1303 gate pulser (gate = 5 ns) and a MCP-gated diode array detector (EG & G Model 1421). The pump and probe beams were focused perpendicularly on a home-made stopped-flow cell which consisted of a capillary (d = 3 mm) of 1 cm path length attached to an airtight 25 mL sample container, to ensure that fresh sample was excited. Operation of this cell was controlled by the OMA program in such a way that the photosensitive sample solution flowed through after each excitation pulse. Picosecond time-resolved absorption spectroscopy was carried out with a system described in detail elsewhere [53,54]. The samples were excited by the second (532 nm) and third (355 nm) harmonic of the Nd:YAG laser with an average pulse energy of 2.5 mJ and a pulse width of approximately 30 ps. The probe pulse was generated by focussing a fraction of the 1064 nm fundamental of the excitation pulse onto D_3PO_4 to give a super-broadened probe pulse covering the 425–675 nm range. A delay line enabled the spectra to be recorded at delays varying from 0 ps to 10 ns after the excitation pulse. The changes in absorbance relative to the spectra measured without the excitation were recorded with an EG & G PAR OMAII console with a silicon-enhanced vidicon array detector. Each spectrum is an average of 6 to 8 recordings. The sample solutions were prepared under nitrogen in a Schlenk tube with attached quartz cuvette (Hellma, 2 mm path length) and were thoroughly mixed between individual excitations. The sample absorbance at the excitation wavelength was kept between 0.3 and 0.5. The time-resolved infrared (TRIR) spectra were collected with a system described elsewhere [30,55]. The 532 nm (fwhm = 10 ns) line of a Nd:YAG laser was used to excite the sample. The output of an infrared diode laser (Mütek MDS 1100) was used as a probe beam. Its frequency was tuned in steps of 4 cm^{-1} between 1880 and 2040 cm^{-1}. The changes in IR absorption at one frequency were monitored with a photovoltaic 77 K HgCdTe detector (Laser Monitoring Systems PV 2180) with a risetime of about 50 ns. The kinetic traces obtained at different wavenumbers were used to construct the IR spectra as a function of time by means of the "point-by-point" method. After each laser flash, the sample solution was made to flow through the cell in order to avoid decomposition of the starting material. Quantum yields of the disappearance of the complexes studied were determined by measuring the decay of their visible absorption band on a Cary 4 E spectrophotometer. The sample was irradiated within the spectrophotometer with one of the laser lines of a SP 2025 Argon-ion laser by an optical fibre and a computer-controlled mechanical shutter. Light intensities were measured with a Coherent model 212 powermeter, which was calibrated with an Aberchrome 540 and 540 P solution according to literature methods [56,57]. The 1 cm cuvette was kept at constant temperature and the solution vigorously stirred during the measurements. The sample concentration was adjusted to keep the maximum absorbance of the MLCT band between 1.5–1.8. The irradiation time intervals were chosen in such a way that the conversion in each irradiation step was less than 5%. The quantum yields reported are average values of several measurements. Typical incident light intensities at the irradiation wavelength were 8–13×10^{-9} einstein s^{-1}. The program used to calculate the quantum yield corrects for changes in the partial absorption of the photoactive compound caused both by its depletion and by the inner filter effect of the photoproduct, by a previously reported procedure [48,58].

Acknowledgements: M. W. George and F. P. A. Johnson at the University of Nottingham (UK) are thanked for measuring the TRIR spectra. B. R. acknowledges C. H. Langford for the opportunity to measure picosecond transient absorption spectra at the Canadian Centre for Picosecond Laser Spectroscopy in Montreal (Canada). The Netherlands Foundation for Chemical Research (SON) and the Netherlands Organization for Pure Research (NWO) are thanked for financial support. Partial support from the Granting Agency of the Czech Republic (203/93/0250) and from the European Research Network and COST programs is also acknowledged.

Received: June 19, 1995 [F153]

[1] D. J. Stufkens, *Comments Inorg. Chem.* **1992**, *13*, 359.
[2] D. J. Stufkens, *Coord. Chem. Rev.* **1990**, *104*, 39.
[3] K. Kalyanasundaram, *Coord. Chem. Rev.* **1982**, *46*, 159.
[4] A. J. Lees, *Chem. Rev.* **1987**, *87*, 711.
[5] K. S. Schanze, D. B. MacQueen, T. A. Perkins, L. A. Cabana, *Coord. Chem. Rev.* **1993**, *122*, 63.
[6] H. K. van Dijk, J. van der Haar, D. J. Stufkens, A. Oskam, *Inorg. Chem.* **1989**, *28*, 75.
[7] T. van der Graaf, D. J. Stufkens, A. Oskam, K. Goubitz, *Inorg. Chem.* **1991**, *30*, 599.
[8] G. J. Stor, M. van der Vis, D. J. Stufkens, A. Oskam, J. Fraanje, K. Goubitz, *J. Organomet. Chem.* **1994**, *482*, 15.
[9] B. D. Rossenaar, T. van der Graaf, R. van Eldik, C. H. Langford, D. J. Stufkens, A. Vlček, Jr., *Inorg. Chem.* **1994**, *33*, 2865.
[10] D. L. Morse, M. S. Wrighton, *J. Am. Chem. Soc.* **1976**, *98*, 3931.
[11] J. C. Luong, R. A. Faltynek, M. S. Wrighton, *J. Am. Chem. Soc.* **1980**, *102*, 7892.
[12] M. W. Kokkes, W. G. J. de Lange, D. J. Stufkens, A. Oskam, *J. Organomet. Chem.* **1985**, *294*, 59.
[13] M. W. Kokkes, D. J. Stufkens, A. Oskam, *Inorg. Chem.* **1985**, *24*, 4411.
[14] M. W. Kokkes, D. J. Stufkens, A. Oskam, *Inorg. Chem.* **1985**, *24*, 2934.
[15] R. R. Andréa, W. G. J. de Lange, D. J. Stufkens, A. Oskam, *Inorg. Chem.* **1989**, *28*, 318.
[16] J. W. M. van Outersterp, D. J. Stufkens, A. Vlček, Jr., *Inorg. Chem.* **1995**, *34*, 5183.
[17] J. W. M. van Outersterp, D. J. Stufkens, J. Fraanje, K. Goubitz, A. Vlček, Jr., *Inorg. Chem.* **1995**, *34*, 4756.
[18] H. A. Nieuwenhuis, A. van Loon, M. A. Moraal, D. J. Stufkens, A. Oskam, K. Goubitz, *Inorg. Chim. Acta* **1995**, *232*, 19.
[19] H. A. Nieuwenhuis, A. van Loon, M. A. Moraal, D. J. Stufkens, A. Oskam, K. Goubitz, *J. Organomet. Chem.* **1995**, *492*, 165.
[20] K. Kaupp, H. Stoll, H. Preuss, W. Kaim, T. Stahl, G. van Koten, E. Wissing, W. J. Smeets, A. L. Spek, *J. Am. Chem. Soc.* **1991**, *113*, 5606.
[21] S. Hasenzahl, H.-D. Hausen, W. Kaim, *Chem. Eur. J.* **1995**, *1*, 95.
[22] J. E. Hux, R. J. Puddephatt, *J. Organomet. Chem.* **1992**, *437*, 251.
[23] P. Bradley, G. Suardi, A. P. Zipp, R. Eisenberg, *J. Am. Chem. Soc.* **1994**, *116*, 2859.
[24] H. A. Nieuwenhuis, D. J. Stufkens, A. Oskam, *Inorg. Chem.* **1994**, *33*, 3212.
[25] H. A. Nieuwenhuis, M. C. E. van de Ven, D. J. Stufkens, A. Oskam, K. Goubitz, *Organometallics* **1995**, *14*, 780.
[26] L. A. Lucia, R. D. Burton, K. S. Schanze, *Inorg. Chim. Acta* **1993**, *208*, 103.
[27] B. D. Rossenaar, D. J. Stufkens, A. Oskam, J. Fraanje, K. Goubitz, *Inorg. Chim. Acta*, in press.
[28] B. D. Rossenaar, C. J. Kleverlaan, D. J. Stufkens, A. Oskam, *J. Chem. Soc. Chem. Commun.* **1994**, 63.
[29] H. A. Nieuwenhuis, D. J. Stufkens, A. Vlček, Jr., *Inorg. Chem.* **1995**, *34*, 3879.
[30] H. A. Nieuwenhuis, D. J. Stufkens, R.-A. McNicholl, J. J. McGarvey, J. Westwell, M. W. George, J. J. Turner, *J. Am. Chem. Soc.* **1995**, *117*, 5579.

[31] B. D. Rossenaar, C. J. Kleverlaan, M. C. E. van de Ven, D. J. Stufkens, A. Oskam, K. Goubitz, J. Fraanje, *J. Organomet. Chem.* **1995**, *493*, 153.
[32] B. D. Rossenaar, M. W. George, F. P. A. Johnson, D. J. Stufkens, J. J. Turner, A. Vlček, Jr., *J. Am. Chem. Soc.* **1995**, *117*, 11582.
[33] L. H. Staal, A. Oskam, K. Vrieze, *J. Organomet. Chem.* **1979**, *170*, 235.
[34] G. J. Stor, F. Hartl, J. W. M. van Outersterp, D. J. Stufkens, *Organometallics* **1995**, *14*, 1115.
[35] R. R. Andréa, W. G. J. de Lange, T. van der Graaf, M. Rijkhoff, D. J. Stufkens, A. Oskam, *Organometallics* **1988**, *7*, 1100.
[36] L. S. Benner, A. L. Balch, *J. Organomet. Chem.* **1977**, *134*, 121.
[37] A. Hudson, M. F. Lappert, P. W. Lednor, J. J. MacQuitty, B. K. Nicholson, *J. Chem. Soc. Dalton Trans.* **1981**, 2159.
[38] S. Terabe, K. Kuruma, R. Konaka, *J. Chem. Soc. Perkin II* **1973**, 1252.
[39] E. G. Janzen, B. J. Blackburn, *J. Am. Chem. Soc.* **1969**, *91*, 4481.
[40] B. D. Rossenaar, D. J. Stufkens, A. Vlček, Jr., *Inorg. Chim. Acta.*, in press.
[41] B. D. Rossenaar, F. Hartl, D. J. Stufkens, submitted for publication in *Inorg. Chem.*
[42] J. C. Luong, R. A. Faltynek, M. S. Wrighton, *J. Am. Chem. Soc.* **1979**, *101*, 1597.
[43] P. C. Servaas, G. J. Stor, D. J. Stufkens, A. Oskam, *Inorg. Chim. Acta* **1990**, *178*, 185.
[44] P. I. Djurovich, R. J. Watts, *Inorg. Chem.* **1993**, *32*, 4681.
[45] P. I. Djurovich, W. Cook, R. Joshi, R. J. Watts, *J. Phys. Chem.* **1994**, *98*, 398.
[46] P. I. Djurovich, R. J. Watts, *J. Phys. Chem.* **1994**, *98*, 396.
[47] D. J. Stufkens, J. W. M. van Outersterp, A. Oskam, B. D. Rossenaar, G. Stor, *Coord. Chem. Rev.* **1994**, *132*, 147.
[48] J. Víchová, F. Hartl, A. Vlček, Jr., *J. Am. Chem. Soc.* **1992**, *114*, 10903.
[49] A. Vlček, Jr., J. Víchová, F. Hartl, *Coord. Chem. Rev.* **1994**, *132*, 167.
[50] The preexponential factor Φ_0 may be simply approximated as $(k_0/k_{nr})\eta_{\sigma\pi^*}$, where k_0 is the preexponential factor of the rate constant for the MLCT $\rightarrow \sigma\pi^*$ conversion, k_{nr} is the rate constant for the deactivation of the MLCT excited state to the ground state (assumed to be temperature-independent) and $\eta_{\sigma\pi^*}$ is the efficiency of the Re–Me bond dissociation from the $\sigma\pi^*$ state, assumed to be about 1 (see text).
[51] R. R. Andréa, D. J. Stufkens, A. Oskam, *J. Organomet. Chem.* **1985**, *280*, 63.
[52] H. Bock, H. tom Dieck, *Chem. Ber.* **1967**, *100*, 228.
[53] C. H. Langford, C. Moralejo, D. K. Sharma, *Inorg. Chim. Acta* **1987**, *126*, 111.
[54] E. Lindsay, A. Vlček, Jr., C. H. Langford, *Inorg. Chem.* **1993**, *32*, 3822.
[55] M. W. George, M. Poliakoff, J. J. Turner, *Analyst* **1994**, *119*, 551.
[56] H. J. Kuhn, S. E. Braslavsky, R. Schmidt, *Pure Appl. Chem.* **1989**, *61*, 187.
[57] H. G. Heller, J. R. Langan, *J. Chem. Soc. Perkin Trans. II* **1981**, 341.
[58] D. M. Manuta, A. J. Lees, *Inorg. Chem.* **1986**, *25*, 1359.

  0947-6539/96/0202-0237 $ 10.00+.25/0